Multiplicity characteristics in relativistic ^{24}Mg-nucleus collisions

A. Abdelsalam[1] E. A. Shaat[1] Z. Abou–Moussa[1] B. M. Badawy[2;1)] Z. S. Mater[1]

[1] Physics Department, Faculty of Science, Cairo University, Egypt
[2] Reactor Physics Department, Nuclear Research Center, Atomic Energy Authority Egypt

Abstract: This work is concerned with the analyses of the shower and gray particle production in 4.5 A GeV/c ^{24}Mg collision with emulsion nuclei. The highest particle production occurs in the region of the low impact parameters. While the multiplicity of the shower particles emitted in the forward direction depends on the projectile mass number and energy, the multiplicity of the backward ones shows a limiting behaviour. The source of the emission of the forward shower particles is completely different from that of the backward ones. The target fragments are produced in a thermalized system of emission.

Key words: ^{24}Mg interactions with emulsion, forward and backward emission of hadrons, projectile and target dependence

PACS: 25.75.-q, 25.75.Dw, 25.75.Gz **DOI:** 10.1088/1674-1137/37/8/084001

1 Introduction

The majority of experiments on high energy nucleon-nucleus and nucleus-nucleus collisions were performed to study the characteristics of multiparticle production in the forward hemisphere (FHS). The particle emission in the backward hemisphere (BHS) attracted much attention from both the theoretical and experimental points of view at the Lawrence Berkeley National Laboratory (LBNL), and JINR [1–3].

In free nucleon-nucleon collision, the backward proton emission is strictly forbidden. The study of the characteristics of the energetic protons emitted in the backward direction through the heavy ion collisions supplies effective information on nuclear effects. In the incident energy range (E<1 GeV per nucleon), Frankel has interpreted the data in terms of the quasi-two-body-scaling model [4], in which the primary mechanism for backward proton productions is a scattering between the incident nucleons and the target nucleons. They are the target nucleons, which are boosted onto the mass-shell and appear in the backward direction. Frankel was able to reproduce the low energy data by a simple structure function and suggested that this function was a measure of the internal momentum distribution of nucleons inside the target. The obtained data show that the characteristic spectrum of the emitted protons with momentum above 400 MeV/c is independent of the projectile type and incident energy. All experimental data [5, 6] about the backward proton characteristics above 2 GeV/nucleon gives evidence for the limiting fragmentation hypothesis, which implies that both the projectile and the target may be fragmented irrespective of each other. Fujita and Hüfner [7] suggested a model for the backward proton emission mechanism, which includes both initial correlations between nucleons in the target and final correlations between two nucleons. The final state interacts with the rest of the target nucleons. Fujita [8] has extended this model to include multiple correlations. The improved model described well the data for the backward proton production at incident energy less than 1 GeV. A theoretical work by Ref. [5] and Ref. [9] indicate that, the backward proton spectra induced by high-energy probes are mainly composed of spectator nucleons from the breakup of correlated pairs in the nucleus. As such, these backward nucleons potentially reflect direct information about the nuclear wave function. Schroeder et al. [1] presented an experiment held at LBNL in order to obtain more information on the mechanisms responsible for high energy backward particle production by bombarding 2.1 GeV proton with various targets. At first, they found a large fraction of events (∼50%) associated with the negative track, which could be identified as a pion. Typically, that pion appeared at $\theta_{\rm lab}$ <90°. Thus, the backward particle emission (typically the backward track is a proton) at 2.1 GeV is often accompanied by the production of a pion. They suggested that the simple quasi-elastic process, NN→NN, as suggested by Frankel [4], was not the dominant mechanism, at that energy for, producing backward protons.

Received 11 May 2012

1) E-mail: he_cairo@yahoo.com

Further information on possible reaction mechanisms could be obtained from a rapidity plot of the positively-charged particles (mostly protons) of those events. There were two suggested possibilities: either, production of a pion followed by its absorption on two target nucleons resulting in two, back-to-back, nucleons, or production of the $\Delta^{++}(1232)$ and its subsequent absorption on a target nucleon via, Δ+N→N+N, resulting in the emission of two protons which would tend to have a near 180° correlation.

On the other hand, the observation of pions beyond the kinematic limit, $\theta_{\rm lab} \geqslant 90°$, had been at Dubna and LBNL [1, 2] on a systematic study of the energy dependence of charged pions produced at 180° in the collisions of 0.8 to 4.89 GeV protons with nuclei. Using 5.14 and 7.52 GeV protons, Baldin et al. [10] observed a charged pion at 180° with energies up to four times larger than expected for free nucleon-nucleon collisions. They stated that the dominant mechanism for producing such pions is on interaction between the incident proton and multinucleon clusters in the target nucleus, referring to this mechanism as "cumulative production". Another experiment was presented by Perdisat et al. [11] using 0.6 GeV protons, in which pions were observed at 155°. The conclusion [11] was that the dominant mechanism is a single scattering, where the incident proton interacts with a target nucleon producing the observed pion via the reaction NN→NNπ. In experiment (10), an exponential energy spectrum for the pions, with a slope parameter $T_0 \approx 60$ MeV, independent of the bombarding energy was found. Another experiment with 28.5 GeV protons [12] studying the backward pion production from a tantalum plate located in the bubble chamber at Brookhaven National Laboratory, BNL, yielded a slope of the energy spectrum consistent with the result of Ref. [10]. Using a combination of data for various backward pion production angles, Baldin reported [10] a similar trend and suggested that it is related to the onset of limiting target fragmentation above 3 GeV.

In this way, the dependence of the backward emission of different particles on the projectile is weaker than that in the forward emission and also the backward emission tends to depend on the target size. At the same time, the characteristics of particles emitted in BHS are completely different from those emitted in a FHS. Therefore, the BHS is intimately connected with the target fragmentation region, i.e. with that part of the phase space where all single particle characteristics are most safe from being dependent on the projectile in accordance with the limiting fragmentation hypothesis when applied to nuclei.

The aim of this paper is to investigate the multiplicity characteristics of the forward and backward shower, gray, and black particles emitted in ^{24}Mg-emulsion interactions at 4.5 A GeV/c. A systematic comparison is made with studies of different projectiles interacting with emulsion nuclei at the same momentum per nucleon.

2 Experimental technique

In this experiment, a stack of nuclear-emulsion-type NIKFI-BR-2 of size 10 cm×20 cm×0.06 cm is used.

This stack was exposed to a 4.5 A GeV/c ^{24}Mg beam at the Dubna Synchrophasotron. The pellicles were doubly scanned along the beam tracks starting from the beam entrance, quickly in the forward direction and coming back slowly to the starting point.

Through a total scanned length of 103.06 meters of beam tracks, 1094 inelastic interactions were observed, such that the experimental mean free path and inelastic interaction cross section are, $\lambda_{\rm exp}$=9.42±0.25 cm and 1330.29±35.80 mb, respectively. These values are found to be in good agreement with the empirical ones deduced using the Bradt-Peters formula following "Glauber's multiple scattering theory" [13].

The tracks of the emitted secondary charged particles in each event were classified according to the traditional emulsion criteria [14] as follows. (a) The shower tracks are singly charged relativistic particles with relative ionization $I/I_0 \leqslant 1.4$, where I is the track ionization and I_0 is the plateau ionization for singly charged minimum ionizing particles. They are mainly pions and their multiplicity is denoted by n_s. (b) The gray tracks have a range of $L \geqslant 3$ mm in emulsion and relative ionization $I/I_0 \geqslant 1.4$. These tracks are mostly due to the recoil target protons with kinetic energy in the range 26–400 MeV. Their multiplicity is denoted by N_g. (c) The black tracks are those having a range of $L < 3$ mm. They correspond to the evaporated target protons with kinetic energy $\leqslant 26$ MeV. Their multiplicity is denoted by N_b. In each event, the black and gray tracks together are called heavily ionizing tracks. Their multiplicity is denoted by ($N_h = N_g + N_b$), and (d) The projectile fragments (PFs) are those emitted with an angle $\theta_{\rm lab} \leqslant 3°$, with respect to the direction of incidence. They are characterized by no change in their ionization for at least 2 cm from the interaction point. The total charge of the stripped fragments in the forward cone per event is denoted by Q. The single charged fragments emitted in the forward fragmentation cone were subjected to rigorous multiple scattering measurements for the momentum determination in order to distinguish them from the produced pions.

3 Results and discussion

3.1 Multiplicity characteristics of secondary particles

This work is devoted to the study of the characteris-

tics of all types of secondary charged particles produced in 4.5 A GeV/c ^{24}Mg-Em inelastic interactions. The present average multiplicity values, $\langle n_{\rm s}\rangle$, $\langle N_{\rm g}\rangle$, $\langle N_{\rm b}\rangle$, and $\langle N_{\rm h}\rangle$ are calculated and compared with the corresponding ones for different projectiles [15–21] at nearly the same incident momentum per nucleon. Table 1 illustrates such comparison which indicates that $\langle n_{\rm s}\rangle$ increases, as expected, with increasing the projectile mass number ($A_{\rm Proj}$). However, the average values of the heavily ionizing particles, $\langle N_{\rm h}\rangle$, appear to be nearly constant for all the compared incident projectiles with $A_{\rm Proj}\geqslant 6$. This could be attributed to the fact that the light projectiles have no sufficient energy to excite the heavy Ag nuclei of the emulsion. The observed constancy of $\langle N_{\rm h}\rangle$, at $A_{\rm Proj}\geqslant 6$ reflects the validity of the limiting fragmentation hypothesis at high energy [3, 22, 23].

Table 1. The average multiplicity values of shower, gray, black, and heavily ionizing particles emitted from the interactions with emulsion nuclei of different projectiles at nearly the same incident momentum per nucleon (4.5 A GeV/c).

projectile	$\langle n_{\rm s}\rangle$	$\langle N_{\rm g}\rangle$	$\langle N_{\rm b}\rangle$	$\langle N_{\rm h}\rangle$	Ref.
p	1.63±0.02	2.81±0.09	3.75±0.08	6.53±0.13	[18]
d	2.77±0.02	3.90±0.10	4.60±0.20	8.50±0.30	[18]
^{4}He	3.37±0.09	3.14±0.12	4.68±0.15	7.82±0.30	[17]
^{6}Li	5.09±0.29	4.23±0.21	4.91±0.30	9.14±0.37	[15]
^{12}C	8.50±0.50	4.60±0.40	4.50±0.30	9.10±0.40	[19]
^{22}Ne	9.98±0.35	5.63±0.24	4.45±0.20	10.08±0.36	[20]
^{24}Mg	10.39±0.27	4.02±0.13	7.00±0.19	11.02±0.30	present work
^{28}Si	12.90±0.40	6.90±0.20	4.70±0.10	11.60±0.13	[21]
^{32}S	13.06±0.45	3.43±0.15	6.72±0.25	10.15±0.40	[16]

Now, it is necessary to investigate the effect of the projectile mass number $A_{\rm Proj}$ on the average multiplicity values of shower and gray particles emitted in both the forward and backward hemispheres, FHS and BHS. For this purpose, the present $\langle n_{\rm s}^{\rm f}\rangle$, $\langle N_{\rm g}^{\rm f}\rangle$, $\langle n_{\rm s}^{\rm b}\rangle$, and $\langle N_{\rm g}^{\rm b}\rangle$ values are listed in Table 2 together with the corresponding results obtained for different projectiles [3, 22–27], having nearly the same incident momentum per nucleon. From this table, one can notice that the average multiplicity of the forward shower particle multiplicity $\langle n_{\rm s}^{\rm f}\rangle$ increases with the increasing of the projectile's size. On the other hand, for projectiles with $A_{\rm Proj}\geqslant 6$, the values of $\langle n_{\rm s}^{\rm b}\rangle$ are nearly constant ($\sim$0.4), which means that the mass number of the incident projectile (in this range) has no effect on the backward shower particle production.

These results strongly support the assumption that while the creation of the forward hadrons is due to the energy transferred from the projectile's participant nucleons, the backward ones originate from a completely different source.

As for the gray particles, the values of both $\langle N_{\rm g}^{\rm f}\rangle$ and $\langle N_{\rm g}^{\rm b}\rangle$ seem to be unaffected by the size of the incident projectile.

3.2 Dependence on the impact parameter

The dependence of the average values of shower, gray, and black particles on interaction centrality degrees is also studied in this work. This degree could be sufficiently indicated by the value of $N_{\rm h}$ [28–31] such that as the interaction becomes more central, the value of $N_{\rm h}$ increases. Consequently, the present interactions are classified into five main groups with $N_{\rm h}$ ranging from 0–1, 2–7, 8–15, 16–27 or $\geqslant$ 28.

Table 3 shows the present average multiplicity values ($\langle n_{\rm s}\rangle$, $\langle N_{\rm g}\rangle$, and $\langle N_{\rm b}\rangle$) at different centrality degrees. According to this table, the average values of shower, gray, and black particles increase with increasing the $N_{\rm h}$ value. When the colliding system moves towards more central regions, the maximum possible number of nucleons presented in the overlapping region between the target and projectile will participate in the interaction. In the overlap region, the colliding objects lose their identity after the collision and form a compound system, which is the source of the secondary charged particles. The relatively large energy and momentum transfers in this region manifest themselves in producing particles, which are isotropically distributed over in the 4π space with large transverse momenta and/or in creating more particles and pions.

Therefore, the highest multiplicities of target fragments and created particles will be obtained at the region of violent (head on) collision, where the overlap region has its maximum size. Such a state can be observed in Table 3 at $N_{\rm h}\geqslant$28, where the complete destruction of AgBr nuclei is expected to occur.

3.3 Forward-backward ratios

Next, we check the effect of both the interaction centrality degree and the projectile mass number, $A_{\rm Proj}$, on the forward-backward ratios for shower and gray

Table 2. The values of the average multiplicities of the shower and gray particles emitted in the FHS and BHS for different interactions.

projectile	incident momentum/(A GeV/c)	$\langle n_{\rm s}^{\rm f}\rangle$	$\langle N_{\rm g}^{\rm f}\rangle$	$\langle n_{\rm s}^{\rm b}\rangle$	$\langle N_{\rm g}^{\rm b}\rangle$	Ref.
p	4.5	1.51±0.01	2.06±0.06	0.11±0.02	0.74±0.04	[3, 22, 23]
^{6}Li	4.5	5.30±0.15	2.08±0.08	0.41±0.01	0.98±0.05	[27]
^{12}C	4.5	7.11±0.02	4.52±0.20	0.45±0.01	1.38±0.07	[24]
^{22}Ne	4.1	9.85±0.04	4.80±0.20	0.45±0.01	1.42±0.08	[25]
^{24}Mg	4.5	10.00±0.27	3.17±0.11	0.40±0.03	0.86±0.05	present work
^{28}Si	4.5	11.36±0.09	4.98±0.18	0.44±0.01	1.42±0.07	[26]
^{32}S	4.5	14.58±0.48	3.17±0.14	0.46±0.01	0.82±0.05	[28]

Table 3. The average values of shower, gray, and, black particles at different centrality degrees (N_h-ranges in 4.5 A GeV/c ^{24}Mg-Em interaction.

N_h-ranges	$\langle n_s \rangle$	$\langle N_g \rangle$	$\langle N_b \rangle$
0–1	4.17±0.33	0.22±0.04	0.31±0.041
2–7	6.00±0.27	1.38±0.07	2.70±0.07
8–15	9.20±0.43	4.00±0.16	7.21±0.20
16–27	16.58±0.48	7.20±0.20	13.47±0.21
⩾28	26.58±1.16	13.85±0.46	13.85±0.46

particles [$(F/B)_s$ and $(F/B)_g$], respectively. Table 4 illustrates that for the first N_h range as well as for the total sample the $(F/B)_s$ increases rapidly with A_{Proj}. At the region of more central collisions, it is concluded by many authors [24, 28, 32–35] that the backward shower particle production is a consequence of a decay of the most high excited target system after the emission of the forward particles and hence, such production depends mainly on the target size. The results shown in Table 4 agree with the previous conclusion where the $(F/B)_s$ ratios decrease with the increase of N_h, i.e. as the interactions become more central, these ratios have their minimum values at $N_h \geqslant 28$. This indicates that the multiplicities of n_s^b attain their greatest values at the most central events. The values of $(F/B)_g$ are found to be nearly around 3.5 irrespective of either the size of the projectile or the impact parameter. This limiting value reflects the isotropy in the behavior of the gray particle emission system in both the forward and backward hemispheres.

Table 4. The forward-backward ratios for different projectiles interacting with emulsion nuclei at different centrality degrees (N_h-values).

projectile		N_h(1–7)	N_h(8–17)	N_h(18–27)	$N_h \geqslant 28$	total sample	Ref.
^{12}C	$(F/B)_s$	44.20	27	22.50	18.50	16.93	[24]
	$(F/B)_g$	4.08	3.41	3.20	3.30	3.51	
^{22}Ne	$(F/B)_s$	48.04	27.54	21.21	16.58	21.89	[25]
	$(F/B)_g$	4.80	3.30	3.10	2.90	3.30	
^{24}Mg	$(F/B)_s$	36.65±5.08	24.58±3.42	21.65±2.69	20.16±2.25	24.95±1.81	present work
	$(F/B)_g$	7.34±1.00	4.00±0.34	3.44±0.25	2.83±0.28	3.70±0.24	
^{28}Si	$(F/B)_s$	62.40	44.04	23.64	17.88	25.82	[25]
	$(F/B)_g$	4.40	3.50	2.90	3.10	3.52	
^{32}S	$(F/B)_s$	95.50	32.53	20.20	21.47	31.76	[26]
	$(F/B)_g$	6.70	3.51	3.06	4.13	3.91	

Table 5 displays the $(F/B)_b$ ratios of the black particle multiplicity observed in the interaction of 4.5 A GeV/c p, ^{3}He, ^{4}He, ^{6}Li, ^{12}C, and ^{24}Mg with emulsion nuclei [36–38]. This table shows that the isotropy factor $(F/B)_b$ has a nearly constant value for all interactions. Therefore, it can be concluded that the system emitting black particles is independent of the projectile mass.

Table 5. The isotropy factor $(F/B)_b$ of the system emitting black particles in 4.5 A GeV/c different projectile interactions with emulsion nuclei.

projectile	$(F/B)_b$	Ref.
p	1.33±0.03	[37]
^{3}He	1.45±0.05	[38]
^{4}He	1.33±0.07	[38]
^{6}Li	1.29±0.06	[36]
^{12}C	1.27±0.10	[37]
^{24}Mg	1.48±0.05	present work

3.4 Target and projectile effects on the backward particle production

In order to study the target and projectile effects on the backward particle production, the present percentage probabilities of the events characterized by the backward emission of shower (n_s^b), gray (N_g^b) and compound ($N_c^b = n_s^b + N_g^b$) particle multiplicities were determined. Table 6 illustrates a comparison between the present results and the corresponding ones for ^{32}S [28] projectile at the same momentum per nucleon. The probabilities of events with $n_s^b > 0$, $N_g^b > 0$, and $N_c^b > 0$ are found to increase with increasing the centrality degree. On the other hand, the probabilities (at different ranges of N_h) seem to be independent of the projectile mass number confirming the previous observation. The percentage of the present events accompanied by the emission, in the BHS, of both shower and gray particles together (i.e. $n_s^b > 0$ and $N_g^b > 0$) was calculated and found to be in agreement with the corresponding values determined for the interactions with emulsion nuclei of 4.5 A GeV/c ^{6}Li [27] and ^{32}S [28]. This indicates that the projectile size has no effect on this percentage. These calculations confirm that the target is the source of the backward particle production (shower and gray) and hence such production is independent of the projectile size. Consequently, it can be concluded from the above experimental data that the backward gray particle may be produced by a different mechanism than that of the forward ones. Such conclusion reveals the existence of the limiting fragmentation hypothesis according to which both the projectile and target may be fragmented irrespective of each other.

Table 6. The probability (in percent) of the interactions accompanied by the emission of shower, gray, and compound particle in the BHS at different impact parameters.

interaction group	projectile	$n_s^b>0$	$N_g^b>0$	$N_c^b>0$	Ref.
$N_h<8$	^{24}Mg	11.90±1.43	13.10±1.50	22.00±1.93	present work
	^{32}S	8.10	14.88	22.47	[28]
$N_h\geqslant 8$	^{24}Mg	41.25±2.83	71.78±3.74	76.65±3.86	present work
	^{32}S	57.00	76.80	84.30	[28]
$N_h\geqslant 28$	^{24}Mg	71.80±9.59	96.15±11.10	97.43±11.18	present work
	^{32}S	73.50	92.64	100	[28]

3.5 Dependence on target size

Now, we investigate the dependence of the average multiplicity of shower particles, $\langle n_s\rangle$, on the target size. For this purpose, it is necessary to consider the composition of the emulsion used. In addition to free hydrogen H, this emulsion contains two groups of nuclei; the light group (CNO) and the heavy one (AgBr). In order to separate the experimental events due to the interactions of the present ^{24}Mg projectile with either hydrogen or a light group or a heavy one, Florian et al's [39] method is used. This method suggests the following.

1) All events due to hydrogen interactions are characterized by N_h=0, 1.

2) The events with $N_h>7$ are interactions with the heavy group (AgBr).

3) The events with $2\leqslant N_h\leqslant 7$ are due to the interactions with the light (CNO) group as well as to the peripheral interactions with the heavy (AgBr) one.

4) The events having $2\leqslant N_h\leqslant 7$ and belonging to the (AgBr) group can be separated by drawing the integral N_h distribution for all events with all values of N_h and then extrapolating this distribution for events with $N_h>7$ in the region of $2\leqslant N_h\leqslant 7$. The extrapolated region would exactly contain a number of events equal to the difference between the total number of events due to the interactions with the heavy (AgBr) group and the number of events having $N_h>7$. Consequently, it becomes easy to determine for each value of N_h, the number of events due to the (CNO) group. The numbers of events, and hence the corresponding percentage, due to H, CNO, and AgBr are obtained from the best fitting of the integral N_h distribution to be (143 events or 13.07%), (356 events or 32.54%) and (595 events or 54.39%), respectively. These values are found to be in good agreement with the corresponding empirical ones calculated according to Ref. [28] [(142, 13%), (354, 32.37%) and (598, 54.65%), respectively].

The present average multiplicities of the shower and heavily ionizing particles emitted in the interaction with hydrogen, light and heavy emulsion nuclei and the corresponding values for ^{12}C [40] and ^{28}Si [22] at the same incident momentum per nucleon are shown in Table 7. One can notice that for a specific target, while the average multiplicity of the heavily ionizing particles, $\langle N_h\rangle$, (which are target fragments) is not affected by the mass number of the incident projectile ($A_{\rm Proj}$), the average multiplicity of the shower particles, $\langle n_s\rangle$, (which are created pions) increases with the increase of $A_{\rm Proj}$. Although the shower particle multiplicity depends mainly in its creation behavior on the projectile mass and energy, however this table, again, confirms that $\langle n_s\rangle$ depends also on the size of the target nuclei. This may be interpreted according to the work of Dabrowska et al [41] who observed a decrease in the number of target fragments having increasing centrality for interactions of projectiles having masses comparable or greater than the mass of the target nucleus. As the collision becomes more central, a significant number of participating protons from the target nucleus get enough momentum to become relativistic due to intranuclear interactions.

Table 8 displays the percentage probabilities of the events characterized by the backward emission of shower, gray, and compound particles multiplicities in the interactions of 4.5 A GeV/c ^{24}Mg with different emulsion components (CNO and AgBr) as well as with the emulsion as a whole. For comparison, the 4.5 A GeV/c ^{32}S corresponding results are also shown in this table.

Table 7. The average values of shower and heavily ionizing particles for different groups of events detected in the interactions with emulsion nuclei of 4.5 A GeV/c ^{24}Mg in comparison with the corresponding results for ^{12}C and ^{28}Si.

projectile	target	$\langle n_s\rangle$	$\langle N_h\rangle$	Ref.
^{12}C	H	0.66±0.05	0.4±0.07	[40]
	CNO	4.80±0.14	2.83±0.12	
	AgBr	10.80±0.19	16.10±0.34	
^{24}Mg	H	3.83±0.31	0.57±0.04	present work
	CNO	5.15±0.20	4.00±0.08	
	AgBr	14.92±0.38	17.75±0.34	
^{28}Si	H	4.77±0.39	0.41±0.03	[22]
	CNO	7.06±0.38	3.77±0.22	
	AgBr	21.29±0.88	17.39±0.72	

Table 8 clarifies that for both 4.5 A GeV/c ^{24}Mg and ^{32}S, the increase of target size has a great effect on the probability of having events accompanied by the emission in the BHS of shower, gray and compound particles. It can also be seen that nearly 30% of the total number of events due to the interaction with emulsion as a whole are characterized by the backward emission of shower particles. This percentage value is consistent with the

Table 8. The probability (in percentage) of the interactions accompanied by the emission of shower, gray and compound particles in the BHS due to different emulsion nuclei.

interaction group	projectile	$n_s^b>0$	$N_g^b>0$	$N_c^b>0$	Ref.
CNO	^{24}Mg	12.64±1.90	12.40±1.86	22.00±2.50	present work
	^{32}S	11.55	18.68	28.75	[28]
Em	^{24}Mg	26.32±1.55	40.70±1.93	47.44±2.08	present work
	^{32}S	30.20	42.80	50.38	[28]
AgBr	^{24}Mg	39.00±1.58	67.23±3.36	73.00±3.50	present work
	^{32}S	44.34	60.64	78.60	[28]

Table 9. The average multiplicities of the shower and gray particles emitted in the FHS and BHS due to the interactions of different projectiles with the CNO and AgBr groups of emulsion nuclei.

interaction group	projectile	$\langle n_s^f\rangle$	$\langle n_s^b\rangle$	$\langle N_g^f\rangle$	$\langle N_g^b\rangle$	Ref.
CNO	^{3}He	2.63±0.07	0.13±0.02	0.91±0.02	0.18±0.01	[38]
	^{4}He	2.97±0.09	0.17±0.02	0.77±0.04	0.18±0.01	[42]
	^{24}Mg	5.01±0.24	0.15±0.02	1.10±0.06	0.14±0.02	present work
	^{32}S	8.91±0.41	0.09±0.02	1.11±0.06	0.16±0.02	[28]
AgBr	^{3}He	5.31±0.12	0.53±0.03	2.63±0.08	0.85±0.03	[38]
	^{4}He	6.70±0.18	0.71±0.05	3.36±0.13	0.93±0.04	[42]
	^{24}Mg	14.54±0.37	0.63±0.05	5.14±0.15	1.49±0.08	present work
	^{32}S	18.15±0.91	0.69±0.02	4.47±0.22	1.23±0.06	[28]

corresponding ones observed in Ref. [10] for ^{6}Li, ^{12}C, and ^{22}Ne at 4.1–4.5 A GeV/c (28.1, 30.2, and 28.04, respectively). This indicates that the probability of interactions having backward relativistic hadrons is nearly independent of the projectile mass number.

The values of the average multiplicity of forward and backward emission of shower and gray particles ($\langle n_s^f\rangle$, $\langle n_s^b\rangle$, $\langle n_g^f\rangle$, and $\langle n_g^b\rangle$, respectively) in the interaction of 4.5 A GeV/c ^{24}Mg (present work), ^{3}He, ^{4}He [38, 41] and ^{32}S [28] with different groups of emulsion nuclei (CNO and AgBr) are listed in Table 9. From this table, one can see that the average number of shower and gray particles in each of the forward and backward hemispheres increases with increasing the target size. This table confirms the conclusion obtained from Table 2 that while the value of $\langle n_s^f\rangle$ depends on the projectile mass number, the value $\langle n_s^b\rangle$ is nearly not affected by $A_{\rm Proj}$. Therefore, it is possible to assume that while the relativistic hadrons flying in the FHS are created as a result of energy transferred from the projectile's participant nucleons, those emitted in the BHS originate from a completely different source.

3.6 Multiplicity distribution of forward and backward particles

The experimental multiplicity distributions of shower and gray particles in both the FHS and BHS [$P(n_s^f)$, $P(N_g^f)$, $P(n_s^b)$, and $P(N_g^b)$, respectively] for the present interaction with CNO, AgBr and emulsion as a whole (Em) are shown in Figs. 1–4. From these figures, one can notice that the distributions of shower and gray particles detected in the FHS [Figs. 1 and 3] extend to much higher multiplicity values than the corresponding distributions in the BHS [Figs. 2 and 4]. This is due to the

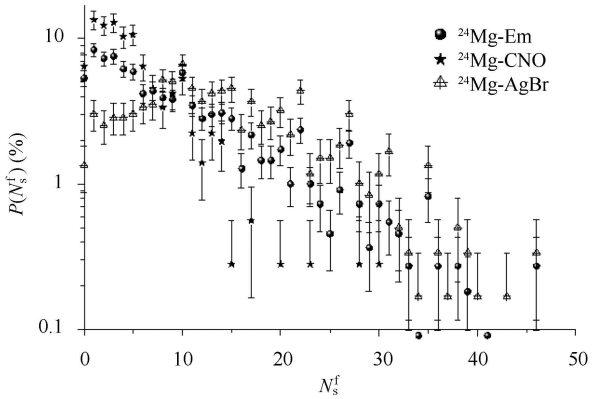

Fig. 1. The normalized multiplicity distributions of shower particles emitted in the FHS due to the interactions of ^{24}Mg with CNO, AgBr, and emulsion at 4.5 A GeV/c.

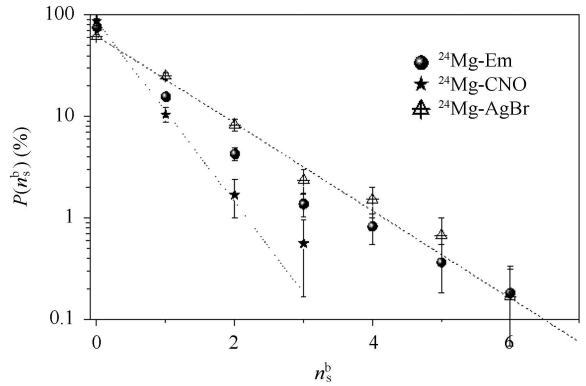

Fig. 2. The normalized multiplicity distributions of shower particles emitted in the BHS due to the interactions of ^{24}Mg with CNO, AgBr, and emulsion at 4.5 A GeV/c, together with the exponential decay lines.

fact that in the FHS the particles are produced with no kinematical restrictions.

The present multiplicity distributions of the backward shower and gray particles can be fitted by the following exponential forms:

$$P(n_{\rm s}^{\rm b})=P_{\rm s}{\rm e}^{-\lambda_{\rm s}^{\rm b}n_{\rm s}^{\rm b}} \text{ and } P(N_{\rm g}^{\rm b})=P_{\rm g}{\rm e}^{-\lambda_{\rm g}^{\rm b}N_{\rm g}^{\rm b}}.$$

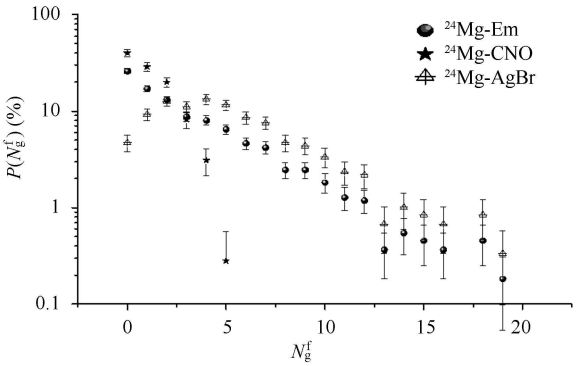

Fig. 3. The normalized multiplicity distributions of gray particles emitted in the FHS due to the interactions of ^{24}Mg with CNO, AgBr, and emulsion at 4.5 A GeV/c.

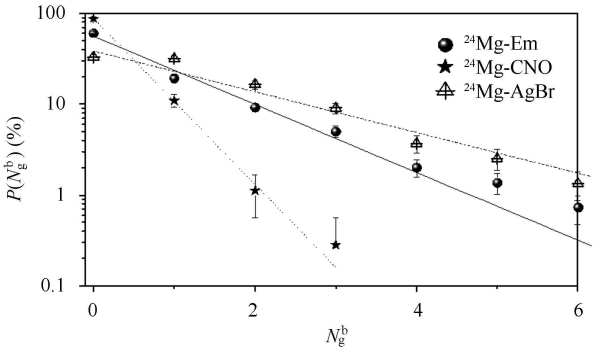

Fig. 4. The normalized multiplicity distributions of gray particles emitted in the BHS due to the interactions of ^{24}Mg with CNO, AgBr, and emulsion at 4.5 A GeV/c, together with the exponential decay lines.

This relation represents the fundamental equation of the decay of an excited system. The decay constants $\lambda_{\rm s}^{\rm b}$ and $\lambda_{\rm g}^{\rm b}$, as obtained from the best fit of the present experimental data, are listed in Table 10 with the corresponding ones for different projectiles [28, 38]. From this table, one can see that for the interaction with emulsion as a whole (Em) the shower particle decay constant $\lambda_{\rm s}^{\rm b}$ seems to be independent of the projectile mass number. This result supports the effective target model [43] where the incident nucleus is assumed to interact with the row of nucleons along its paths and hence excite them, in a collective fashion. During the de-excitation, the emission of pions occurs in a manner similar to that in the thermal models. Such conclusion is also consistent with the model drawn by Fredriksson [44] according to which the incident nuclei interact collectively with all matter within 1 fm (in the rest frame) at the line of collision. On the other hand, the value of the decay constant $\lambda_{\rm s}^{\rm b}$ decreases with increasing the target size. The relationship between the gray decay constant $\lambda_{\rm g}^{\rm b}$ and both the projectile mass number and target size are observed to be similar to those for the shower decay constant $\lambda_{\rm s}^{\rm b}$. The above results for the shower and gray particles emitted in the BHS confirm the limiting fragmentation hypothesis at the incident momentum used. Therefore, the shower particles, which are flying above the kinematic limit (in the BHS), may be thought to be due to the decay of an exciting system (cluster) at a fixed temperature in the first step. Then the backward gray particles are expected to be emitted in the second step.

3.7 Comment

In the light of the above results of the backward emitted shower and gray particles, we would like to outline the following.

Our group, (Mohamed El-Nadi High Energy Lab, Faculty of Science, Cairo University, Egypt), carried out a series of experiments [24–28, 32, 33, 35–38, 45–47] investigating backward relativistic hadron production. The results show that those hadrons are not created particles. Their production system is a decay system characterized by a decay constant $\lambda\sim$1.3 for emulsion target nuclei. The temperature of this system is $T\sim$27 MeV. Such hadrons depend mainly on the target size at the region of limiting fragmentation.

The pion production in relativistic pA and AA collisions was investigated recently by Abdelsalam et al. [46]. In that experiment, a wide range of projectiles, with mass numbers ($A_{\rm Proj}$=1 to 32), was used at Dubna energy. The pion production was examined underlying their zonal emission influence at the FHS and the BHS. The study reveals that the forward emitted pions are expected to result from a system of particle creation through a fireball nuclear matter or hadronic matter decay. Otherwise, the backward emitted pions result from an exact decay system of excited target nucleus in a later stage after the production of forward ones.

In Experiment [47], ^{32}S collisions with emulsion nuclei, at two widely separated beam energies of 3.7A and 200 A GeV are studied to examine the behavior towards hadronization process. In Experiment [48], the same interactions are utilized to examine the target size dependence in the production of the forward and backward emitted relativistic hadrons in the framework of the Lund Monte-Carlo program code-events generating FRITIOF

Table 10. The fitting parameters of the backward shower and gray particle distributions, which are fitted by an exponential decay form.

projectile	target	λ_s^b	P_s	λ_g^b	P_g	Ref.
^{12}C	Em	1.09±0.04	63.22±7.75	0.75±0.06	45.92±11.56	[32]
^{22}Ne	Em	1.06±0.04	58.52±6.98	0.66±0.04	40.91±7.58	[32]
	Em	1.17±0.04	74.55±2.28	0.86±0.04	55.89±2.13	
^{24}Mg	CNO	2.05±0.03	86.89±4.92	2.10±0.03	87.72±4.92	present work
	AgBr	0.99±0.05	62.26±3.01	0.52±0.08	40.00±2.03	
^{28}Si	Em	1.02±0.08	54.93±13.14	0.67±0.04	42.11±8.88	[32]
	Em	1.05±0.05	62.67±7.06	0.76±0.02	50.88±5.23	
^{32}S	CNO	2.38±0.10	86.86±11.22	1.81±0.04	83.07±6.64	[28]
	AgBr	0.89±0.05	61.68±6.97	0.67±0.03	52.77±7.68	

model [49–51]. The results suggest that the forward emitted shower particles originate from a source, which is different from that responsible for the backward shower particle production.

The present study confirms the above-observed results. Since the production of the relativistic hadrons is suggested to be from two different sources according to the emission direction of these hadrons, the present emission systems may be described in the light of the multi source ideal gas model ([52, 53] and references therein). Fu-Hu Liu [52], Fu-Hu Liu and Jun-Sheng Li [53] introduced their model assumption that many sources of emitted particles are formed in the collisions of e^+e^-, pp, $p\overline{p}$, e^+p, pA, and AA. The authors of Ref. [52, 53] could give a formula, which describes uniformly the multiplicity distributions of final state particles produced in the mentioned collisions at high energy. The model also can be used to describe the particle emission angles. In the algorithm description of this model [52–54], the multiplicity (n_{ij}) distribution contributed by the $i^{\rm th}$ source in the $j^{\rm th}$ group is an exponential function of the form,

$$P_{ij}(n_{ij})=\frac{1}{\langle n_{ij}\rangle}\exp\left(-\frac{n_{ij}}{\langle n_{ij}\rangle}\right).$$

This formula can be compared with the produced exponential decay laws describing the data of Fig. 2 and Fig. 4 for the backward emitted shower and gray particles, respectively. Hence, to draw a complete picture of our systems of particle emission sources, it may be preferable to consider a subsequent study in the framework of the multi source thermal model.

4 Conclusion

On the basis of the present study of ^{24}Mg-Em interaction at 4.5 A GeV/c, the following can be obtained:

1) The average multiplicity values of the forward shower particles, $\langle n_s^f\rangle$ (which are mostly created pions) increase with the increase of projectile's size (i.e. with the increase of the number of the projectile's interacting nucleons). On the other hand, the values of $\langle n_s^b\rangle$ are nearly independent of the projectile size ($\langle n_s^b\rangle\approx 0.4$, starting from ^{6}Li).

2) The values of both $\langle N_g^f\rangle$ and $\langle N_g^b\rangle$ seem to be unaffected by the size of the incident projectile.

3) The average multiplicity value of shower particles increases with the increase of the target size.

4) The ratio $(F/B)_s$ increases rapidly with the mass number of the projectile. At the regions of more central collisions (i.e. those with the highest N_h values), the multiplicities of n_s^b will attain their greatest values, thus they contribute more to $(F/B)_s$. Accordingly, the value of $(F/B)_s$ is found to decrease gradually by a factor of at least ∼1.2 as the centrality increases. This decrement factor shows constancy with the projectile mass number at $N_h\geqslant 28$ (complete destruction of Ag and Br nuclei).

5) The values of $(F/B)_g$ are found to be nearly around 3.5 irrespective of the change of the projectile or the impact parameter. This limiting value reflects the isotropy in the behavior of the system emitting gray particles in both FHS and BHS.

6) The $(F/B)_b$ ratios of the black particle multiplicity have a constant value for different projectiles. Therefore, this ratio is considered as an isotropically factor for the system exciting evaporated particles.

7) The probabilities of events with $n_s^b>0$, $N_g^b>0$ and $N_c^b>0$ are found to increase with increasing the centrality degree. On the other hand, the probabilities (at different ranges of N_h) seem to be independent of the projectile mass number.

8) The percentage of the present events accompanied by the emission, in the BHS, of both shower and gray particles together (i.e. $n_s^b>0$ and $N_g^b>0$) was calculated and found to agree with the corresponding values determined for 4.5 A GeV/c ^{6}Li [25] and ^{32}S [14]. This indicates that the projectile size has no effect on this percentage, i.e., the target is the source of the backward particle production of shower with gray particles.

9) The backward emitting gray particles may be produced by a different mechanism from that of the forward ones.

10) As the target size increases, the average number

of shower particles in each of the forward and backward hemispheres increases.

11) The multiplicity distributions of shower and gray particles detected in the FHS (see Figs. 1 and 3) extend to higher values than the corresponding distributions in the BHS (see Figs. 2 and 4). This is due to the fact that the particles produced in the FHS result from the contributions of both projectile and target participates while in the BHS, the target size is the only affecting parameter.

12) The results presented in this work strongly support the assumption that while the creation of the forward hadrons is due to the energy transferred from the projectile's participant nucleons, the backward ones originate from a completely different source.

This work was carried out at the Mohamed El-Nadi High Energy Physics Laboratory, Physics Department, Faculty of Science, Cairo University, Egypt.

The authors would like to thank all the staff of (Vekseler and Baldin) High Energy Laboratory at JINR, Dubna, Russia, for providing us with the irradiated emulsion plates.

References

1 Schroeder L S et al. Phys. Rev. Lett., 1979, **43**: 1787
2 Burgov N A et al. Sov. J. Nucl. Phys., 1987, **45**: 463
3 Abdelsalam A, Šumbera M, Vokál S. JINR, El–82–509; Dubna, 1982
4 Frankel S. Phys. Rev. Lett., 1977, **38**: 1338
5 Frankfurt L L, Strikman M I. Phys. Lett. B, 1979, **83**: 497
6 Bayukov Y D et al. Phys. Rev. C, 1979, **20**: 764
7 Fujita T, Hufner J. Nucl. Phys. A, 1979, **314**: 317
8 Fujita T. Nucl. Phys. A, 1979, **324**: 409
9 Yukawa T, Furui S. Phys. Rev. C, 1979, **20**: 2316
10 Baldin A M et al. Sov. J. Nucl. Phys., 1975, **20**: 629
11 Perdrisat C F, Frankel S, Frati W. Phys. Rev. C, 1978, **18**: 1764
12 Papp J et al. Phys. Rev. Lett., 1975, **34**: 601
13 Glauber R J. Lectures in Theoretical Physics. Vol. 1, Interscience, New York: 1959, 315; Glauber R J. High Energy Physics and Nuclear Structure. North-Holland, Amsterdam, 1967, 315; Glauber R J. High Energy Physics and Nuclear Science. North-Holland, Amsterdam, 1969, 202
14 Powell C F, Fowler F H, Perkins D H. The Study of Elementary Particles by the Photographic Method. Pergamon Press. London, New York: Paris, Los Angles, 1958, 474
15 Sherif M M. Egypt. J. Phys., 1992, **23**: 55
16 Fayed M, Thesis M Sc. Faculty of Science. Cairo University, 1997
17 Tolostov K. D. JINR Preprint, Dubna., 1974, **8313**: 1
18 Barashenkov V S et al. Yad. Fiz., 1981, **33**: 1061
19 Mansy M M. Thesis M Sc. Cairo University Faculty of Science, Phys. Dept. 1982
20 Ahmed N R. Ph D Thesis. submitted to the Faculty of Science Cairo University, Egypt, 1988
21 Adamovich M I et al. Communication of the Joint Institute for Nuclear Research. Duban E1–92–569, 1992
22 Bannik B P et al. Czech. J. Phys. B, 1981, **31**: 490
23 Bubnov V I et al. Z. Phys. A, 1981, **303**: 133
24 El-Nadi M, Ali-Mossa M N, Adedelsalam A. IL Nuovo Cimento A, 1998, **110**: 1255
25 El-Nadi M, Ali-Mossa N, Adedelsalam A. Int. J. Mod. Phys. E, 1994, **3**: 811
26 El-Nadi M, Abedelsalam A, Ali-Moussa N. Radiat. Phys. Chem., 1996, **47**: 681
27 El-Nadi M, Abdelsalam A, Ali-Mossa N, Abou-Moussa Z, Abdel-Waged Kh, Osman W, Badawy B M. IL Nuovo Cimento A, 1998, **111**: 1243
28 Abdelsalam A, Shaat E A, Ali-Mossa N, Abou-Mousa Z, Osman O M, Rashed N, Osman W, Badawy B M, El-Falaky E. J. Phys. G, 2002, **28**: 1375
29 Jain P L et al. Phys. Rev. Lett., 1987, **59**: 2531
30 Adamovich M I et al. Eur. Phys. J. A, 1998, **1**: 77
31 Abedelsalam A. JINR Report (Dubna), 1981, E1-81-623
32 Abdelsalam A, Badawy B M, El-Falaky E. Can. J. Phys., 2007, **85**: 837
33 Abedelsalam A et al. JINR Report (Dubna), P1-83-577 in Russian, 1983
34 Badawy B M. J. Nucl. Rad. Phys., 2008, **3**: 31
35 Badawy B M. Int. J. Mod. Phys. E, 2009, **18**: 648
36 El-Nadi M, Abdelsalam A, Ali-Mossa N, Abou-Moussa Z, Kamel S, Abdel-Waged Kh, Osman W, Badawy B M. Eur. Phys. J. A, 1998, **3**: 183
37 Abdelsalam A, El-Nagdy M S, Rashed N, Badawy B M. Chinese Journal of Physics, 2007, **45**: 351
38 Abdelsalam A et al. Egypt. J. Phys., 2005, **36**: 257
39 Florian J R; (Alma-Ata Leningrad, Moscow. Tashkent Collaboration, Lebedev Institute), preprint Moscow, 1974, 9
40 Bodarenko R A et al. Yad. Fiz., 1983, **38**: 1483 in Russian
41 Dabrowska A et al. Nucl. Phys. A, 2001, **693**: 777
42 Abdelsalam A, El-Nagdy M S, Rashed N, Badawy B M, El-Falaky E. Journal of Nuclear and Radiation Physics, 2007, **2**: 49
43 Mathis H B, MENG Ta-Chung. Phys. Rev. C, 1978, **18**: 952
44 Fredrikson S. Royal Inst. Tech. Preprint TRITA-IFY 80-6, Stockholm, Sweden, 1980
45 Abdel-waged K. Phys. Rev. C, 1999, **59**: 2792
46 Abdelsalam A, El-Nagdy M S, Badawy B M. Can. J. Phys., 2011, **89**: 261
47 Abdelsalam A, Badawy B M, Hafiz M. Can. J. Phys., 2012, **90**: 515
48 Abdelsalam A, Badawy B M, Hafiz M. J. Phys. G, 2012, **39**: 105104
49 Andersson B, Gustafson G, Nilsson-Almqvist B. Nucl. Phys. B, 1987, **281**: 289
50 Nilsson-Almquist B, Stenlund E. Comp. Phys. Comm., 1987, **43**: 387
51 EMU01 Collaboration. Z. Phys. A, 1997, **358**: 337
52 LIU Fu-Hu. Nucl. Phys. A, 2008, **810**: 159
53 LIU Fu-Hu, LI Jun-Sheng. Phys. Rev. C, 2008, **78**: 044602
54 Rahim M A, Fakhraddin S, Asharabi H. Eur. Phys. J. A, 2012, **48**: 115